Chemosphere 203 (2018) 199–208

Contents lists available at ScienceDirect

Chemosphere

journal homepage: www.elsevier.com/locate/chemosphere

# Differential behaviors of silver nanoparticles and silver ions towards cysteine: Bioremediation and toxicity to *Phanerochaete chrysosporium*

Zhenzhen Huang [a, 1], Zhuotong Zeng [b, 1], Anwei Chen [c, 1], Guangming Zeng [a, *], Rong Xiao [b, **], Piao Xu [a], Kai He [a], Zhongxian Song [d], Liang Hu [a], Min Peng [a], Tiantian Huang [a], Guiqiu Chen [a]

[a] College of Environmental Science and Engineering, Hunan University and Key Laboratory of Environmental Biology and Pollution Control (Hunan University), Ministry of Education, Changsha, 410082, PR China
[b] Department of Dermatology, Second Xiangya Hospital, Central South University, Changsha, 410011, PR China
[c] College of Resources and Environment, Hunan Agricultural University, Changsha, 410128, PR China
[d] School of Municipal and Environmental Engineering, Henan University of Urban Construction, Pingdingshan, 467036, PR China

## HIGHLIGHTS

- Bioremediation and AgNP/$Ag^+$ toxicity were dependent on Cys:Ag ratio to some extent.
- More stability in Ag uptake was induced by cysteine under stress of $Ag^+$ than AgNPs.
- Cysteine supply aggravated or marginally mitigated ROS level under AgNP/$Ag^+$ stress.
- Distinction was related to lability and bioavailability of Ag-cysteine complexes.

## GRAPHICAL ABSTRACT

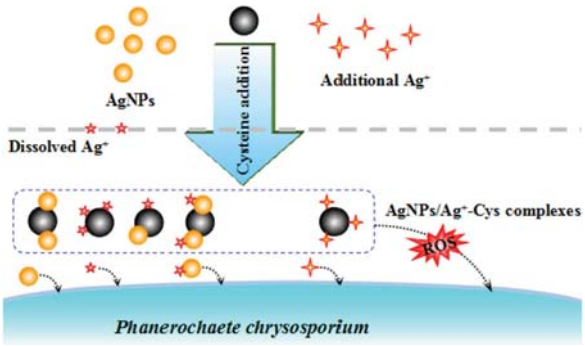


## ARTICLE INFO

*Article history:*
Available online 21 March 2018

Handling Editor: Tamara S. Galloway

*Keywords:*
Cysteine
Silver nanoparticles
Silver ion
*Phanerochaete chrysosporium*
Bioremediation
Toxicity

## ABSTRACT

Potential transformations of silver nanoparticles (AgNPs) upon interaction with naturally ubiquitous organic ligands in aquatic environments influence their transport, persistence, bioavailability, and subsequent toxicity to organisms. In this study, differential behaviors of AgNPs and silver ions ($Ag^+$) towards cysteine (Cys), an amino acid representative of thiol ligands that easily coordinate to $Ag^+$ and graft to nanoparticle surfaces, were investigated in the aspects of bioremediation and their toxicity to *Phanerochaete chrysosporium*. Total Ag removal, 2,4-dichlorophenol (2,4-DCP) degradation, extracellular protein secretion, and cellular viability were enhanced to some extent after supplement of various concentrations of cysteine under stress of AgNPs and $Ag^+$. However, an obvious decrease in total Ag uptake was observed after 5–50 μM cysteine addition in the groups treated with 10 μM AgNPs and 1 μM $Ag^+$, especially at a Cys:Ag molar ratio of 5. More stabilization in uptake pattern at this ratio was detected under $Ag^+$ exposure than that under AgNP exposure. Furthermore, in the absence of cysteine, all $Ag^+$ treatments stimulated the generation of reactive oxygen species (ROS) more significantly than high-dose AgNPs did. However, cysteine supply under AgNP/$Ag^+$ stress aggravated ROS levels, albeit alleviated at

* Corresponding author.
** Corresponding author.
*E-mail addresses:* zgming@hnu.edu.cn (G. Zeng), xiaorong65@csu.edu.cn (R. Xiao).
[1] These authors contribute equally to this article.

https://doi.org/10.1016/j.chemosphere.2018.03.144

100 μM $Ag^+$, indicating that the toxicity profiles of AgNPs and $Ag^+$ to *P. chrysosporium* could be exacerbated or marginally mitigated by cysteine. The results obtained were possibly associated with the lability and bioavailability of AgNP/$Ag^+$-cysteine complexes.



## 1. Introduction

Silver-based nanomaterials are one of the most widely used noble metal nanomaterials due to their relatively low-cost, unique optical, electrical, photocatalytic, physicochemical, and antimicrobial properties (Siriwardana et al., 2015a; Zhang et al., 2015a, b, 2016; Yuan et al., 2016). Silver nanoparticles (AgNPs) have been increasingly applied in numerous fields, such as consumer products, medical supplies and equipment, water treatment, electrochemical sensing, and biosensing (Navarro et al., 2008; Kanel et al., 2015; Xu et al., 2012a; Gong et al., 2009; Deng et al., 2013; Zhang et al., 2015a, b). Due to the widespread use of AgNPs, their inevitable release into the environment leads to the nanoparticles being a source of dissolved Ag (Xiu et al., 2012), which would cause adverse effects to natural microbial communities, such as bacteria (Guo et al., 2016a; Priester et al., 2014), fungi (Guo et al., 2016b; He et al., 2017; Yi et al., 2016), and algae (Navarro et al., 2015), potentially resulting in a significant impact on aqueous ecosystems (Dobias and Bernier-Latmani, 2013; Chen et al., 2015; Cheng et al., 2016; Tan et al., 2015). The transport, fate, and ecological implications of AgNPs are largely affected by the complexity of the aquatic system such as pH, ionic strength, and natural organic matter (NOM), as well as the properties of nanoparticles (Long et al., 2011; Ellis et al., 2016; Tang et al., 2014).

Given the ubiquity of NOM in aquatic systems, substantial studies have focused on how organic materials influence the bioavailability and toxicity of AgNPs (Aiken et al., 2011). For example, organic matters or metal-binding ligands can induce a change in surface charges or steric effects of nanomaterials, thus influencing their adsorption to inorganic surfaces and interaction with biological membranes (Yang et al., 2014; Wan et al., 2017). Moreover, organic coatings appear to modify the surface of nanoparticles, causing dispersion or aggregation of AgNPs with implications for their bioavailability (Wirth et al., 2012; Stoiber et al., 2015). Similarly, AgNP dissolution will increase dissolved Ag concentration, which in turn affects the adsorption and desorption kinetics of ligands (Gondikas et al., 2012). Some sulfhydryl-containing organic compounds such as glutathione, phytochelatins, and cysteine (Cys) can effectively chelate silver ions ($Ag^+$) released from nanomaterials, resulting in the unavailability of Ag to exposed organisms (Yang et al., 2014). Xiu et al. (2011) found that the addition of cysteine completely counteracted the toxicity of $Ag^+$ to *Escherichia coli* (*E. coli*). Similarly, Guo et al. (2016a, b) explored the strong and concentration-dependent excitation of cysteine to *E. coli* cells when 12.5 mg/L cysteine was added into AgNP suspensions at concentrations of 1.7–5.1 mg/L. Although it has been suggested that cysteine, a major low-molecular-weight thiol, can slow down AgNP coagulation, aggravate the dissolution of AgNPs, and induce a hormesis effect of nanoparticles in a concentration-dependent manner (Xiu et al., 2011; Guo et al., 2016a; Gondikas et al., 2012), studies on the influence of cysteine on bioremediation of microorganisms exposed to AgNPs are not investigated in detail.

The main goal of this work was to define the effects of thiol-containing ligands (cysteine) on Ag removal and 2,4-dichlorophenol (2,4-DCP) degradation from aquatic settings by *Phanerochaete chrysosporium* (*P. chrysosporium*) under stress of AgNPs/$Ag^+$. Cysteine, a thiol containing amino acid with better-defined structure than humic macromolecules, was selected because of its wide application in toxicity assessments of AgNPs to infer the bioavailability and effects of dissolved $Ag^+$. To further identify the difference between AgNP- and $Ag^+$-induced cytotoxicity during fungal remediation processes, dissolved $Ag^+$ concentration, extracellular protein content, cellular viability, and reactive oxygen species (ROS) generation were monitored in the presence and absence of cysteine.

## 2. Materials and methods

### 2.1. AgNP synthesis and characterization

AgNPs coated with citrate were synthesized according to the procedure as described in our previous publication (Huang et al., 2017, 2018). Briefly, 59.5 mL solution containing 0.6 mM trisodium citrate and 1.8 mM sodium borohydride ($NaBH_4$, >99% purity, Sigma Aldrich) was prepared with ultrapure water (18.25 MΩ·cm) and vigorously stirred under ice bath conditions. And then 0.5 mL $AgNO_3$ (24 mM) was added into the mixture. After agitation at room temperature for 3 h, the prepared AgNP suspensions were purified by using a 1 kDa regenerated cellulose membrane to remove the excess reactants, such as trisodium citrate and $Ag^+$. Size (hydrodynamic diameters) and zeta-potential of AgNPs were measured with dynamic light scattering (DLS) method using a Malvern Zetasizer Nano-ZS (Malvern Instrument, U.K.). Transmission electron microscopy (TEM, JEOL JEM-3010, Hitachi Corporation, Japan) sample was prepared via drying out few drops of the cleaned AgNP suspension onto copper grids coated with a continuous carbon support film at room temperature. All chemicals used were at least of analytical reagent grade.

### 2.2. Microorganism

*P. chrysosporium* strain BKMF-1767 (CCTCC AF96007), as the model species of white-rot fungi, was purchased from the China Center for Type Culture Collection (Wuhan, China) and maintained on potato dextrose agar slants at 4 °C. *P. chrysosporium* spore suspension was prepared by gently scraping the spores from the agar surface into sterile ultrapure water. After the concentration of the spore suspension being adjusted to $2.0 \times 10^6$ CFU/mL, the fungal spore suspensions were inoculated into the culture medium and cultivated at 37 °C and 150 rpm in an incubator.

### 2.3. Effects of incubation period and exposure time

3 mL of spore suspension was added into 500 mL conical flasks containing 200 mL culture medium and cultured under different incubation periods (60 and 72 h). Then, *P. chrysosporium* pellets were harvested and rinsed for the succeeding experiments of exposure time in three ways: (1) the fungi incubated for 72 h were further exposed to 10 μM AgNPs and 20 mg/L 2,4-DCP for 2 h; (2) the fungi incubated for 60 h were further treated with AgNPs and 2,4-DCP at the same doses for 2 h; and (3) the fungi incubated for

60 h were further treated with the same concentrations of AgNPs and 2,4-DCP for 12 h. After 2 and 12 h of exposure to AgNPs and 2,4-DCP, aliquot samples were taken at pre-decided intervals (1, 3, 6, 9, 12, 24, 36, 48, 60, 72, 84, 96, and 108 h). Effects of incubation period (60 and 72 h) and exposure time (2 and 12 h) of *P. chrysosporium* on bioremediation were assessed by determining the performance of total Ag removal and 2,4-DCP degradation, as well as the dissolution of AgNPs.

### 2.4. Silver-cysteine complexation experiments

Complexation experiments were carried out to assess potential effects of cysteine concentrations (5–5000 μM) on 2,4-DCP degradation, total Ag removal, and AgNP dissolution in the AgNP toxicity experiments. Prior to addition of various concentrations of cysteine, AgNPs and 2,4-DCP were added to the aqueous solutions at the initial concentrations of 10 μM and 20 mg/L, respectively. After pre-equilibration for 10 min (time for reaching equilibrium of silver-cysteine complexes), the harvested *P. chrysosporium* pellets, which were cultivated for 3 days and rinsed several times with 2 mM sodium bicarbonate buffer (Xiu et al., 2011, 2012), were added to the mixtures. The samples were taken out at different time intervals and centrifuged in a centrifuger (TGL20-M, Hukang, China) at 10,000 × g for 10 min. The supernatants were used for analysis of the residual total Ag, dissolved $Ag^+$, and 2,4-DCP concentrations. Likewise, toxicity response of $Ag^+$ (using $AgNO_3$ as $Ag^+$ source) in the presence of cysteine was performed in the same conditions except for the substitution of 10 μM AgNPs with 1 μM $AgNO_3$. Besides, influences of cysteine on removal and degradation performance of *P. chrysosporium* were estimated at high concentrations of AgNPs (60 and 100 μM) and $Ag^+$ (30 and 100 μM) with a Cys:Ag molar ratio of 50. In contrast, the mycelia were also exposed to various concentrations of AgNPs and $Ag^+$ without cysteine to investigate single AgNP or $Ag^+$ cytotoxicity.

### 2.5. Protein quantification

Alterations in extracellular proteins were determined under different incubation time, exposure time, and cysteine concentrations in the presence of AgNPs or $Ag^+$, and their contents were quantified by the Coomassie Brilliant Blue method using a UV–vis spectrophotometer (Model UV-2550, Shimadzu, Japan) at 595 nm (Huang et al., 2015, 2017).

### 2.6. Assessment of cell viability

Cell viability assay was carried out by using 3-(4,5-dimethylthiazol-2-yl)-2,5-diphenyl tetrazolium bromide (MTT) uptake and reduction according to Chen et al. (2014). MTT, a yellow water-soluble tetrazolium dye, can be reduced by living cells to a water-insoluble purple formazan. The MTT conversion occurs only in living cell mitochondria and is directly related to the number of metabolically viable cells. After exposure to the solutions containing AgNPs or $AgNO_3$, *P. chrysosporium* pellets (0.2 g) were added into MTT solution (1 mL; 5 mg/mL). After cultivation of 2 h at 50 °C, the reaction was terminated with the addition of HCl solution (0.5 mL; 1 M) to the mixture. Then, the MTT-containing mixture was centrifuged at 4 °C (10,000 × g, 5 min) and the supernatant was decanted. Subsequently, the pellets were mixed with 6 mL of propan-2-ol under agitation for 2 h at 25 °C. The absorbance was recorded at 534 nm with a UV–vis spectrophotometer. In the experiment, the viability of *P. chrysosporium* was expressed as a percentage relative to the control (100%; untreated with AgNPs, $Ag^+$, 2,4-DCP, or cysteine).

### 2.7. Measurement of ROS

Intracellular ROS levels induced under stressed conditions were examined using the cell permeable indicator, 2′,7′-dichlorodihydrofluorescein diacetate ($H_2$DCF-DA; Sigma), which was hydrolyzed to the non-fluorescent compound 2′,7′-dichlorodihydrofluorescein ($H_2$DCF) by intracellular esterase upon entering the cells (Chen et al., 2014; Hu et al., 2017). $H_2$DCF would be rapidly oxidized to the highly fluorescent 2′,7′-dichlorofluorescein (DCF) in the presence of the intracellular ROS. Thus, the DCF fluorescence intensity of the supernatant was measured using a FluoroMax-4 fluorescence spectrometer (Horiba Scientific, Tokyo, Japan) with excitation at 485 nm and emission at 525 nm. In the test, *P. chrysosporium* pellets were stained in the culture medium containing 5 μM $H_2$DCF-DA for 2 h following 24-h exposure to the indicated concentrations of AgNPs and $Ag^+$ with or without cysteine. The staining medium was then discarded, and the stained cells were rinsed with phosphate-buffered saline (PBS) three times prior to homogenization and centrifugation. The fluorescence intensity of DCF indicated the extent of the intracellular ROS generation.

### 2.8. Analytical procedure

The removal amounts of Ag and 2,4-DCP from aqueous solutions were calculated as the differences between the initial concentrations of the added AgNPs/$AgNO_3$ and 2,4-DCP and the final concentrations of total Ag and 2,4-DCP in the filtrates. Total Ag concentrations (including AgNPs and $Ag^+$) in the solutions were evaluated by using a flame atomic absorption spectroscopy (FAAS, PerkinElmer AA700, USA). Prior to the FAAS measurements, the samples were digested with $HNO_3$ and $H_2O_2$ as previously described (Xiu et al., 2011). Dissolved $Ag^+$ concentrations in the stock solutions were determined by filtration of stock solutions through ultrafiltration centrifuge tube (1 kDa) using an inductively coupled plasma-optical emission spectrophotometer (ICP-OES, IRIS Intrepid II XSP, Thermo Electron Corporation, USA). The concentration of 2,4-DCP in the filtrate was quantitated by using high performance liquid chromatography (Agilent 1100 series HPLC; Agilent Technologies; Wilmington, DE) as described earlier by our team (Huang et al., 2015). Briefly, the column temperature was maintained 35 °C with UV detection at 287 nm. The elution was carried out with an isocratic mobile phase of acetonitrile/water (80:20, v/v) at a flow rate of 1.0 mL/min. The supernatant was filtered through a 0.45-μm PVDF membrane syringe filter. 20 μL of the filtrate was injected into an Agilent Eclipse Zorbax XDB column (150 × 4.6 mm, 5 μm) proceeded by a C18-type guard column.

Each assay treatment was carried out in triplicate, and all of the data were presented as the arithmetic mean value with the standard deviation of at least three individual measurements. The results obtained were analyzed by using Origin Pro 9.0 software (OriginLab, Northampton, MA). Statistical analyses were also performed to evaluate the statistical differences between the treatment groups during the experiments with the IBM SPSS statistical software package for Windows, version 19.0 (IBM Corporation, Armonk, New York, USA), according to One-way analysis of variance (ANOVA) followed by a Student-Newman-Keuls post-hoc test. Differences at the level of $p < 0.05$ were considered to be statistically significant.

## 3. Results and discussion

### 3.1. AgNP characterization

The resulting AgNP suspension (20.01 mg/L) was primarily

composed of spherical particles with an average particle diameter of 13.5 (±7.6) nm in basis of TEM observations (Fig. 1). The average hydrodynamic diameter of AgNPs was also estimated with the value of 22.6 (±2.5) nm. Inconsistency in size distributions determined by TEM and DLS methods resulted from their different measurement principles (Guo et al., 2016a). The zeta-potential of AgNPs showed a negative value of −11.3 (±1.7) mV, and the dissolved fractions of AgNP suspensions were found to be less than 1%.

### 3.2. Effects of incubation period and exposure time on total Ag removal, AgNP dissolution, and 2,4-DCP degradation

The effects of incubation period and exposure time on total Ag removal, AgNP dissolution, and 2,4-DCP degradation by *P. chrysosporium* are shown in Fig. 2. It can be seen from Fig. 2a that the maximum removal percentages were 79.17%, 92.5%, and 100% for 12 h of exposure at the incubation time of 60 h, 2 h of exposure at the incubation time of 72 and 60 h, respectively. The total Ag removal amounts for 2-h exposure were greatly higher than those for 12-h exposure after 36–72 h of sampling time, possibly due to long-term exposure to AgNPs and 2,4-DCP causing chronic damage and even cell death (Zhou et al., 2018; Chen et al., 2014). As for short-term exposure (2 h) to AgNPs and 2,4-DCP, a higher total Ag removal was obtained for a 72-h-old cultivation with the maximum removal rate of 100%. It suggested that a 72-h-old cultivation was greatly beneficial for the growth, reproduction, and metabolism activity of *P. chrysosporium*. However, no significant difference in 2,4-DCP degradation was observed when the incubation period of *P. chrysosporium* varied in the range of 60–72 h and the exposure time increased from 2 to 12 h (Fig. 2c), which was possibly because a low concentration of 2,4-DCP (20 mg/L) could be used as carbon and energy sources during the total Ag removal process (Huang et al., 2015, 2017; Liang et al., 2017; Wu et al., 2017).

It is well-known that $Ag^+$ ions are released from AgNPs under acidic conditions through oxidizing the nanoparticles in aqueous solutions exposed to air (Equation (1))

$$4Ag^0 + O_2 + 4H^+ \rightarrow 4Ag^+ + 2H_2O \quad (1)$$

In addition to dissolved oxygen and pH values of solutions, the release of $Ag^+$ was related to the metabolic state of *P. chrysosporium*. Fig. 2b shows that different incubation periods and exposure time lead to obvious difference in the release pattern of $Ag^+$. Maximum concentrations of dissolved $Ag^+$ were up to 0.47 and 0.36 μM when *P. chrysosporium* was exposed to AgNPs and 2,4-DCP for 2 h at the incubation time of 60 and 72 h, respectively. However, relatively low levels of $Ag^+$ (≤1 μM) were found to enhance the biological activity and fitness of microbe, and stimulate Ag removal and 2,4-DCP degradation as previously reported (Huang et al., 2017). Meanwhile, little change in dissolved $Ag^+$ levels was observed under 12 h of exposure, which could be associated with microbial metabolites. For example, extracellular proteins boosted the repulsive force among nanoparticles through inducing a charge to the particle surface, and organic acids could block the available binding sites and impede the continual leaching of AgNPs after adherence to the surface of nanoparticles (Zuo et al., 2015). Taken together, the release of $Ag^+$ was remarkably inhibited at a lower level after long-term exposure when compared with that after short-term exposure.

### 3.3. Effect of initial cysteine concentration on 2,4-DCP degradation

2,4-DCP degradation was enhanced after the addition of cysteine in AgNP- and $Ag^+$-treated groups, especially in those following high-dose exposure (Fig. 3). At the low AgNP concentration (e.g. 10 μM), an obvious increase in 2,4-DCP degradation percentage was observed in the presence of cysteine from 1 to 48 h relative to that untreated with cysteine (Fig. 3a). Furthermore, it has been previously demonstrated that Ag-cysteine polymers/particles are expected to be formed particularly at low ratios of Cys:Ag (≤5), without the formation of particulate Ag for a Cys:Ag ratio of 50 (Gondikas et al., 2012). Thus, AgNP/$Ag^+$-cysteine mixtures were formulated with the molar ratio of 50 to impede the formation of Ag-cysteine polymers/particles in this study. Notably, the supplied cysteine modulated the biodegradation of 2,4-DCP more effectively at high AgNP concentrations with this ratio. The maximum degradation rates of 2,4-DCP in 60 and 100 μM AgNP-treated groups increased from 84.8% to 73.4%–100%, respectively, without and with cysteine. Likewise, an increase of 77.1% in 2,4-DCP degradation rate was caused by addition of cysteine after exposure to 30 μM $Ag^+$ as compared to that under the stress of $Ag^+$ alone without cysteine (22.6%), and for the given $Ag^+$ concentrations of 100 μM, the maximum degradation rate of 2,4-DCP in the absence of cysteine was 21.9%, which was also increased to 100% on account of the supply of cysteine (Fig. 3b). Cysteine, typically found in natural waters (e.g., wastewater, surface waters, and sediment porewater) at low levels (nanomolar to micromolar range), is a very strong metal-complexing agent, capable of preferential binding of $Ag^+$ to the sulfur groups of this organic thiol (Gondikas et al., 2012; He et al., 2012; Zhang et al., 2004). Moreover, cysteine was been found to have little influence on cell growth (in section 3.6). It was speculated that formation of Ag-cysteine complexes could lower the levels of free $Ag^+$, inhibit Ag uptake, and alleviate the overall cytotoxicity of AgNPs and/or $Ag^+$ (Navarro et al., 2015), further improving the biodegradation of 2,4-DCP. However, as for a low $Ag^+$ concentration (1 μM), the supplied cysteine of 5 and 50 μM appeared not to distinctly influence 2,4-DCP degradation; even a decrease in 2,4-DCP degradation was obtained when 500 μM cysteine was supplied in the solution. This might be attributed to

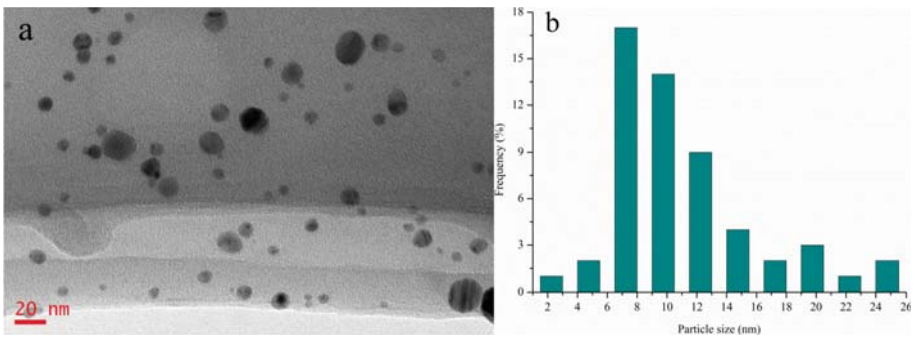


**Fig. 1.** Characterization of as-prepared AgNPs: (a) representative TEM micrograph and (b) histogram of measured particle sizes from (a).

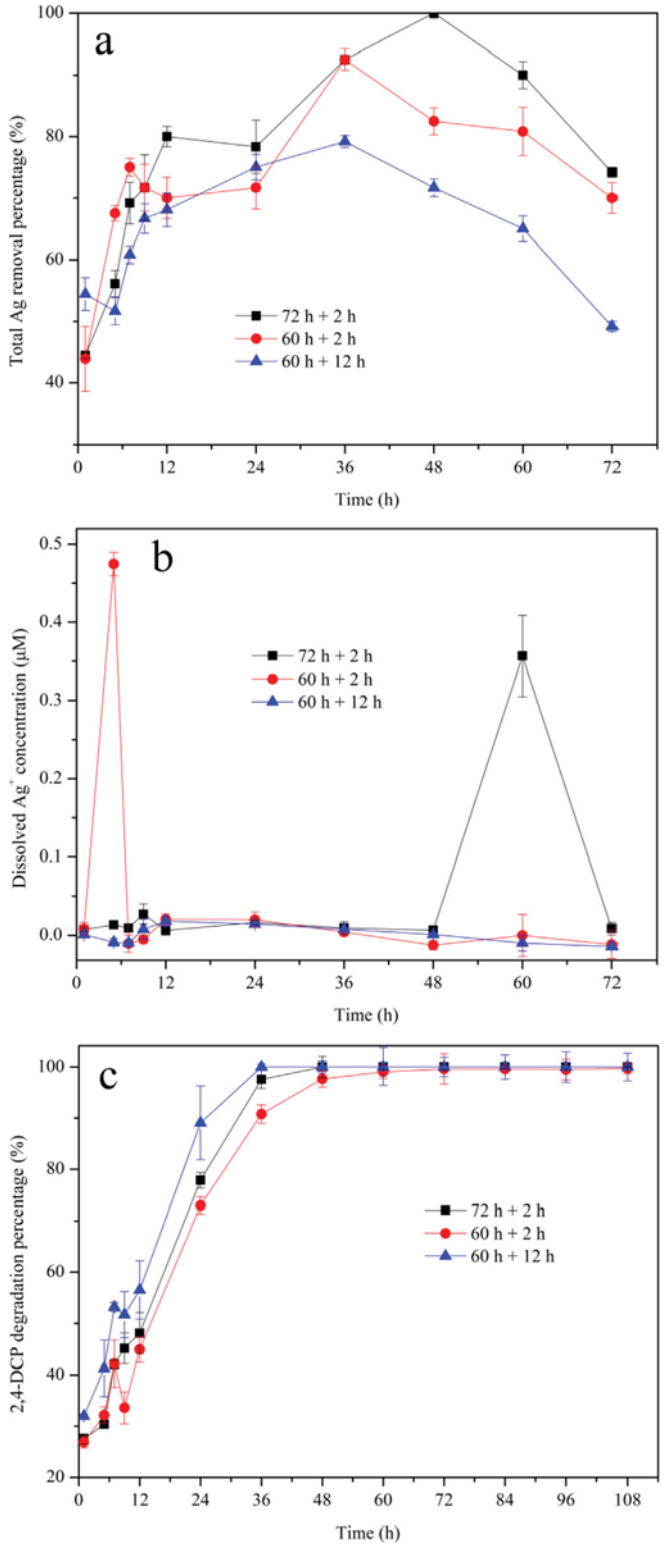


**Fig. 2.** Effects of incubation period (60 and 72 h) and exposure time (2 and 12 h) on (a) total Ag removal, (b) AgNP dissolution, and (c) 2,4-DCP degradation.

the difference in Cys:Ag ratio leading to different bioavailabilities in Ag-cysteine species. Partial soluble Ag-cysteine species readily taken up by *P. chrysosporium* probably resulted in a decline in 2,4-DCP degradation to some extent.

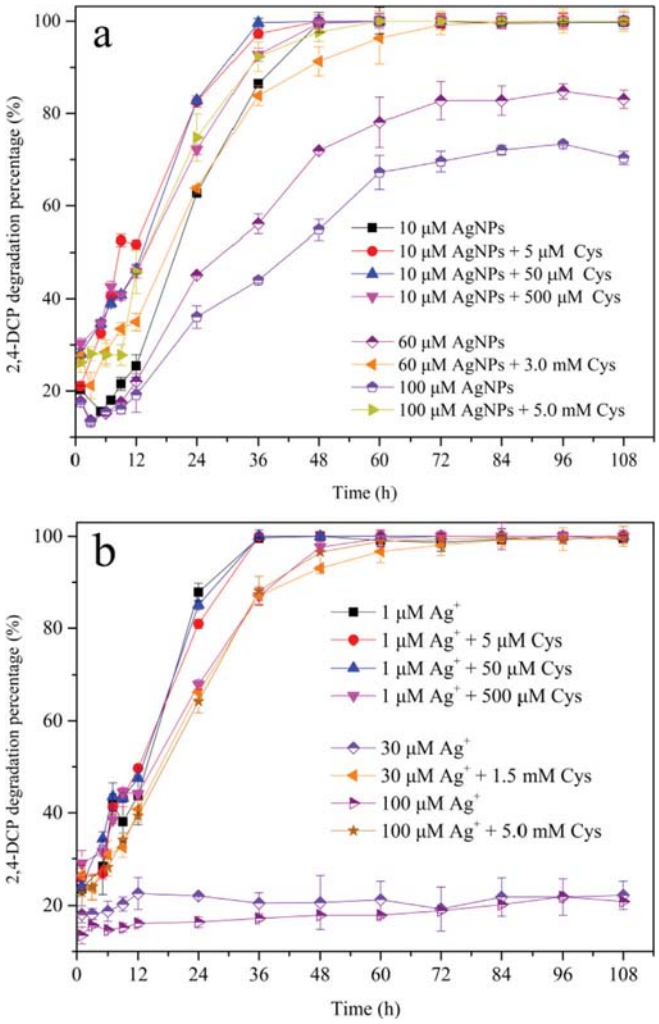


**Fig. 3.** Cysteine enhanced 2,4-DCP degradation by *P. chrysosporium* under the treatments with (a) AgNPs and (b) $Ag^+$.

### 3.4. Effect of initial cysteine concentration on total Ag removal

Cysteine ranging from 5 to 5000 μM resulted in different effects on total Ag removal under the treatments with AgNPs and $Ag^+$ (Fig. 4). Patterns of total Ag uptake within 24 h were similar to those of 2,4-DCP degradation within 48 h upon AgNP exposure in the presence of cysteine, showing higher removal rates than those in the group treated with AgNPs without cysteine (Fig. 4a). A tentative explanation was that after short-term treatment with cysteine, the zeta-potential of AgNPs could be shifted to less negative values, causing more total Ag removal relative to the treatment without cysteine (Huang et al., 2018; Wang et al., 2016; Eckhardt et al., 2013). Interestingly, a remarkable decline in total Ag removal was detected when cysteine came into contact with 10-μM AgNP-treated cells for 36 h. Afterwards, total Ag removal percentage under 500 μM cysteine rapidly increased from 59.2% to 98.3%, which was higher than that under just 10 μM AgNPs (the maximum of 96.1%); however, there was a substantial reduction in total Ag uptake after supplement of low concentrations of cysteine (5 and 50 μM), eventually dropping to 48.3% and 39.2%, respectively, at 72 h. A similar trend as for AgNPs was observed for 1 μM $Ag^+$ in total Ag uptake with cysteine in the range of 5–500 μM (Fig. 4c). Almost complete removal of total Ag was obtained after exposure to 1 μM $Ag^+$ with and without 500 μM cysteine (99.9% and 99.6%,

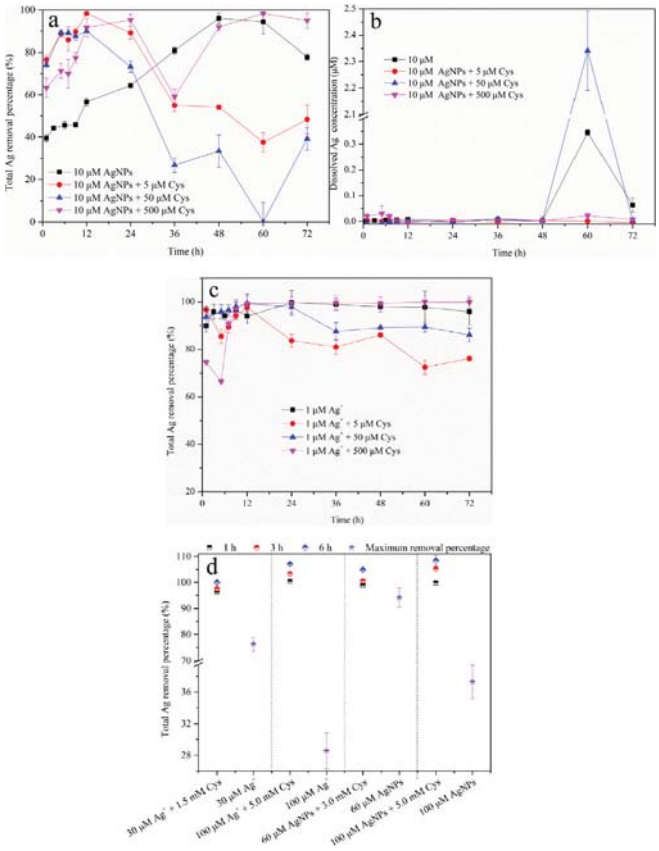


**Fig. 4.** Effects of cysteine on total Ag removal at (a) 10 μM AgNPs, (c) 1 μM $Ag^+$, and (d) high concentrations of AgNPs and $Ag^+$. (b) Dissolved $Ag^+$ concentrations measured in solutions under various cysteine levels.

respectively). Nevertheless, a decline in total Ag uptake was achieved under 1 μM $Ag^+$ treatments with 5 and 50 μM cysteine over 12 h.

It should be noted that the total Ag uptake rates under exposure to 10 μM AgNPs and 1 μM $Ag^+$ were both declined after addition of 5 and 50 μM cysteine. The minimum uptake rates of total Ag under AgNP/$Ag^+$ exposure were obtained at a Cys:Ag ratio of 5, and the changing pattern in total Ag uptake under $Ag^+$ exposure was more stable with higher uptake rates than that under AgNP exposure at this ratio. The findings implied that a more complex role of cysteine might be played in the medium including AgNPs in contrast to $Ag^+$. It is well-known that cysteine can not only strongly bind and remobilize $Ag^+$, but also influence the aggregation, dissolution, and surface charge of AgNPs by adherence onto their surfaces (Gondikas et al., 2012; Afshinnia et al., 2016; Hu et al., 2016; Navarro et al., 2015). Such processes therefore potentially resulted in the greater instability in Ag uptake due to the unstable Ag-cysteine complexes in the context of AgNPs. For example, cysteine at a low concentration (the Cys:Ag ratio of 0.5) could be only chelated with part of the dissolved $Ag^+$ released from AgNPs to form Ag-cysteine complexes that promoted AgNP aggregation to certain extent, resulting in a decline in total Ag uptake at this ratio. When cysteine was added far in excess of Ag concentrations (Cys:Ag ≥ 50), Ag-cysteine complexes formed with higher coverage of AgNPs/$Ag^+$ with cysteine slowed the dissolution and aggregation of AgNPs. Meanwhile, the complexes might be directly adsorbed onto the surface of cells and/or penetrated into them, due to the abundant peptides, polysaccharides, and pigments existing on the hyphae or micropinocytosis and caveolae-mediated endocytosis (Ren et al., 2017; Xu et al., 2012b; Hu et al., 2017). It was obvious that higher ratios of Cys:Ag led to higher Ag removal rates. Nevertheless, at a Cys:Ag ratio of 5, it was hypothesized that Ag-cysteine complexes might be the major sinks driving equilibrium Ag biopartitioning (Liu et al., 2010). Higher cysteine concentrations than total Ag doses probably resulted in the following two cases: (1) complexation of cysteine with dissolved $Ag^+$ facilitated the dissolution of nanoparticles (Siriwardana et al., 2015a); and (2) additional free cysteine molecules were available for interaction with AgNP surfaces inducing aggregation of the nanomaterials, as previously reported by Gondikas et al. (2012). These could be the factors that gave rise to the instability of total Ag removal. As seen in Fig. 4b, the concentration of dissolved $Ag^+$ at the Cys:AgNPs molar ratio of 5 is indeed significantly enhanced with respect to only AgNP treatment without cysteine, indicating an enhancement in AgNP dissolution at this Cys:Ag ratio. However, little change in dissolved $Ag^+$ concentrations was observed at very low levels when the ratios of cysteine to AgNPs were 0.5 and 50. The observations were in agreement with the findings of total Ag removal in Fig. 4a, which suggested that total Ag removal was closely related to the ratios of Cys:Ag.

Additionally, the influence of cysteine on total Ag removal was also investigated at high concentrations of AgNPs and $Ag^+$ with a Cys:Ag ratio of 50 (Fig. 4d). In the absence of cysteine, maximum removal percentages of total Ag were 76.3%, 28.5%, 94.2%, and 37.3% under the treatments with 30 and 100 μM $Ag^+$, 60 and 100 μM AgNPs, respectively, suggesting that $Ag^+$ exerted a more potent toxic effect on *P. chrysosporium* than AgNP did on basis of total silver concentration. However, the total Ag removal rates reached almost 100% upon the addition of cysteine for 1 h, and slightly increased at 3 and 6 h. Although the supplied cysteine induced a substantial increase in total Ag removal, especially at high concentrations of $Ag^+$ and AgNPs, the contribution of $Ag^+$ versus the AgNPs themselves to higher toxicity of AgNPs to fungi was not discerned during this process. Consequently, influences of cysteine on extracellular protein secretion, cellular viability, and ROS generation were investigated under AgNP and $Ag^+$ exposure in the following sections.

### 3.5. Effect of cysteine on extracellular protein content

Our previous study has demonstrated that the toxic effects of AgNPs/$Ag^+$ may be related to their interactions with proteins (Huang et al., 2015; Zuo et al., 2015). In the present study, the contents of extracellular proteins secreted by *P. chrysosporium* increased within 12 h and subsequently decreased with sampling time to some extent under treatments of 10 μM AgNPs or 1 μM $Ag^+$ with 20 mg/L 2,4-DCP (Tables 1–3). In terms of exposure time, the concentrations of extracellular proteins secreted for 12 h of exposure were generally higher than those for 2-h exposure (Table 1). Coupled with the changes in extracellular protein contents during various exposure time and sampling time, it was assumed that short-term contact with AgNPs and 2,4-DCP (within 12 h of exposure time and sampling time) probably induced up-regulation of protein contents in response to adverse environmental factors, whereas the decline in protein secretion after further contact for 24–72 h could be explained by the disturbance of chronic damage in the biosynthesis of proteins (Chen et al., 2014; Khojasteh et al., 2016). Another possibility for the decrease in extracellular protein content was that these proteins might subsequently be utilized as nitrogen sources by *P. chrysosporium* pellets to enhance their biological activity, further facilitating Ag removal and 2,4-DCP degradation (Huang et al., 2015, 2017). Similar phenomena on the reduction of extracellular protein secretion were observed in Tables 2 and 3 after long-term contact with AgNPs and $Ag^+$ in the

**Table 1**
Changes in extracellular protein content (μg/mL) under different incubation time and exposure time at 10 μM AgNPs and 20 mg/L 2,4-DCP.

| Culture conditions | 1 h | 3 h | 6 h | 9 h | 12 h | 24 h | 36 h | 48 h | 60 h | 72 h |
|---|---|---|---|---|---|---|---|---|---|---|
| 72 h + 2 h | 72.85 | 78.99 | 81.58 | 79.79 | 86.73 | 69.13 | 66.00 | 68.53 | 68.48 | 65.67 |
| 60 h + 2 h | 70.54 | 76.03 | 77.23 | 76.67 | 84.63 | 66.25 | 65.59 | 66.33 | 67.60 | 68.21 |
| 60 h + 12 h | 75.18 | 79.28 | 79.65 | 79.24 | 83.82 | 71.76 | 68.82 | 71.78 | 74.30 | 75.05 |

72 and 60 h are incubation time and 2 and 12 h are exposure time.

**Table 2**
Changes in extracellular protein content (μg/mL) at different concentrations of cysteine in the presence of 10 μM AgNPs and 20 mg/L 2,4-DCP.

| 10 μM AgNPs + Cys concentration | 1 h | 3 h | 6 h | 9 h | 12 h | 24 h | 36 h | 48 h | 60 h | 72 h |
|---|---|---|---|---|---|---|---|---|---|---|
| 0 μM Cys | 71.67 | 68.45 | 69.91 | 70.76 | 71.87 | 75.36 | 71.57 | 68.78 | 66.46 | 68.40 |
| 5 μM Cys | 71.68 | 76.71 | 80.79 | 80.34 | 75.59 | 64.31 | 63.23 | 64.39 | 65.05 | 61.99 |
| 50 μM Cys | 72.93 | 76.54 | 79.20 | 79.48 | 79.20 | 64.45 | 63.53 | 64.70 | 64.54 | 62.32 |
| 500 μM Cys | 71.53 | 75.93 | 79.44 | 78.75 | 77.99 | 62.14 | 62.03 | 62.58 | 62.62 | 60.69 |

**Table 3**
Changes in extracellular protein content (μg/mL) at different concentrations of cysteine in the presence of 1 μM $Ag^+$ and 20 mg/L 2,4-DCP.

| 1 μM $Ag^+$ + Cys concentration | 1 h | 3 h | 6 h | 9 h | 12 h | 24 h | 36 h | 48 h | 60 h | 72 h |
|---|---|---|---|---|---|---|---|---|---|---|
| 0 μM Cys | 71.60 | 71.44 | 72.77 | 72.81 | 65.61 | 64.91 | 63.74 | 65.22 | 67.69 | 68.43 |
| 5 μM Cys | 71.09 | 74.74 | 78.65 | 79.17 | 79.89 | 68.70 | 63.72 | 64.59 | 65.38 | 64.67 |
| 50 μM Cys | 71.23 | 73.50 | 75.89 | 75.88 | 79.57 | 63.76 | 63.76 | 65.47 | 67.30 | 67.69 |
| 500 μM Cys | 72.11 | 76.35 | 77.64 | 77.84 | 81.14 | 64.62 | 62.36 | 62.85 | 62.31 | 59.04 |

presence of cysteine. Besides, the maximum content of extracellular protein (86.73 μg/mL) related to different incubation time was obtained when *P. chrysosporium* cells were exposed to AgNPs and 2,4-DCP for 2 h at the incubation time of 72 h. This demonstrated that 72-h incubation was instructive for fungal colonization, further greatly improving the removal of toxicants, which was in accordance with the results in Fig. 2a.

On the basis of investigations on influence of varying concentrations of cysteine on the secretion of extracellular proteins under the stress of AgNPs, it was found that the significant increments in extracellular protein production were induced by various cysteine concentrations (5, 50, and 500 μM) in the first 12 h, up to 80.79, 79.48, and 79.44 μg/mL, respectively, which were higher than that induced by AgNPs alone with the maximum of 75.36 μg/mL (Table 2). The similarity of alteration in the concentrations of extracellular proteins secreted was observed under $Ag^+$ stress in the presence and absence of cysteine (Table 3). Stimulation of cysteine on extracellular protein production within 12 h could be closely related to the potential association of reactivity of $Ag^+$ and AgNPs themselves with the added cysteine (Siriwardana et al., 2015b). AgNP/$Ag^+$-cysteine complex formation avoided the direct contact of AgNPs/$Ag^+$ with extracellular proteins, whereas lack of cysteine caused interplay of AgNPs/$Ag^+$ with extracellular fungal proteins via chemical cross-linking or electrostatic force of attraction, leading to some conformational changes of the proteins (Navarro et al., 2015; Khan et al., 2011). These could also be the cause of the observed higher concentrations of extracellular proteins under AgNP/$Ag^+$ stress with cysteine at 1–12 h than those without cysteine. Another factor may be the higher cell densities stimulated by cysteine treatment (further explained in Section 3.6), which may contribute to greater secretion of extracellular proteins (Khojasteh et al., 2016). However, extracellular protein secretion in concentration-response curves over sampling time (24–72 h) showed an opposite trend, with slightly higher values for the samples without addition of cysteine than those with cysteine supply. Although upon cysteine addition, the formation of AgNPs/$Ag^+$-cysteine complexes occurred, the structure and conformation of the complexes may change with exposure time during the process of metabolism of *P. chrysosporium*, which possibly depressed the secretion of extracellular protein (Siriwardana et al., 2015b). Furthermore, there is no obvious dependence between the impacts of cysteine on extracellular protein contents and the Cys:Ag ratios.

### 3.6. Action of cysteine on cellular viability

For further discerning the cytotoxicity of AgNPs versus $Ag^+$, impacts of cysteine on the viability of *P. chrysosporium* were investigated following exposure to AgNPs and $Ag^+$ with various concentrations of cysteine (0–50 mM) for 24 h. Results showed that cysteine enhanced the stimulatory effects of AgNPs and $Ag^+$ on *P. chrysosporium* cells to some extent (Fig. 5). As shown in Fig. 5a, cysteine addition resulted in a significant enhancement in cellular viability of *P. chrysosporium* under high-dose AgNP stress (60 and 100 μM) relative to the groups treated with AgNPs alone, while an insignificant difference in cellular viability was observed between the control, the just cysteine groups, and the 10 μM AgNP-treated groups with and without cysteine. In contrast, in the presence of 1 μM $Ag^+$, cellular viability was significantly stimulated when cysteine was administered at the concentrations of 50 and 500 μM (28.8% and 25.8% higher than that of the just 1-μM $Ag^+$-treated cells, respectively) (Fig. 5b). However, further increase in $Ag^+$ concentrations (≥10 μM) caused obvious toxic effects on *P. chrysosporium* in a concentration-dependent manner, leading to cell death with approximately 41.0%, 71.5%, and 78.6% of the total cells at $Ag^+$ concentrations of 10 μM, 1, and 10 mM, respectively, in the absence of cysteine. Some studies indicate that cysteine can isolate the effect of AgNPs and decrease $Ag^+$ availability (Navarro et al., 2008; Xiu et al., 2011), dramatically decrease the inhibitory effects of $Ag^+$ in a concentration-dependent manner, and even completely mitigate the toxicity of AgNPs and $Ag^+$ (He et al., 2012). In marked contrast to these studies, cysteine addition in the range of 5–500 μM appeared not to effectively modulate the microbicidal properties of $Ag^+$ at 10 μM, 1, and 10 mM with the maximum increases in cellular viability of 10.6%, 14.9%, and 11.4%, respectively, in comparison with those without cysteine. It was hypothesized

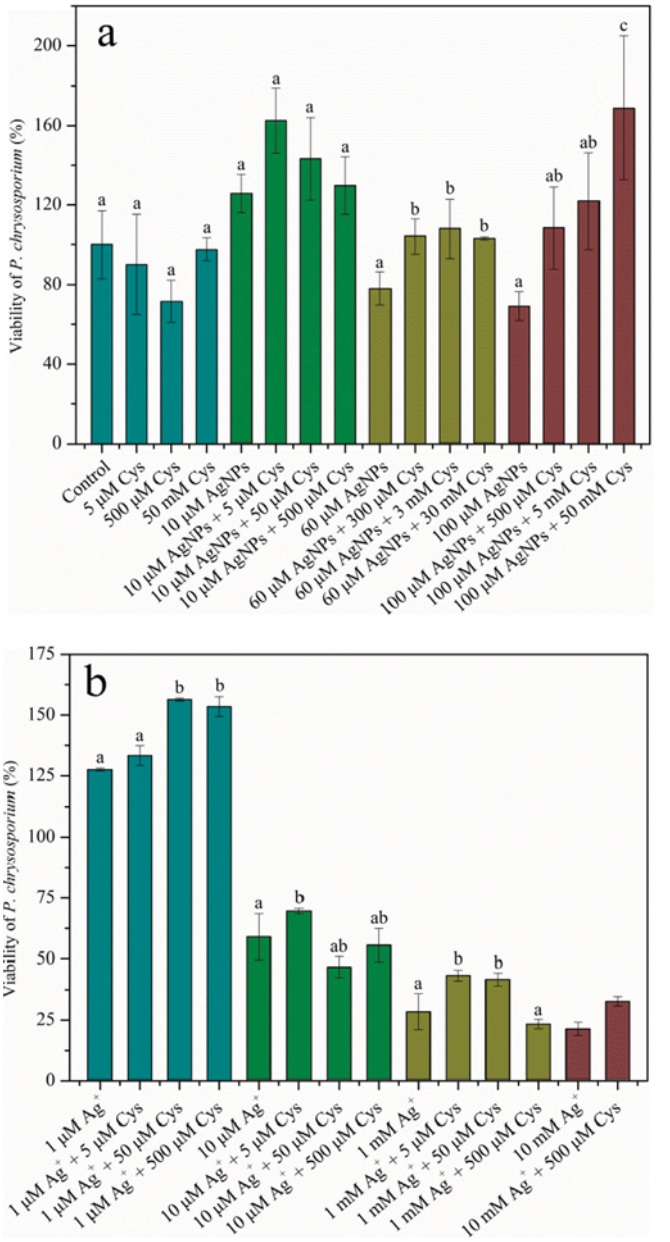


**Fig. 5.** Viability of *P. chrysosporium* upon exposure to (a) AgNPs and (b) $Ag^+$ with and without various concentrations of cysteine.

that the deleterious effects of $Ag^+$ on *P. chrysosporium* in the presence of cysteine were likely due to limited binding of $Ag^+$ by cysteine under these conditions, or that the cysteine-bound Ag species could be sufficiently labile for $Ag^+$ release, resulting in $Ag^+$ still being bioavailable and readily taken up by this fungus (Luoma et al., 2016; Fabrega et al., 2009). These results were consistent with those for the marginally mitigating influence of cysteine addition on $Ag^+$ toxicity to phytoplankton as previously reported (Lodeiro et al., 2017).

### 3.7. Effect of cysteine on ROS levels

Substantial studies point out that the mechanism underlying AgNP-induced toxic effects and the antibacterial activity of $Ag^+$ ions are strongly associated with ROS generation (Huang et al., 2016; Massarsky et al., 2014; Li et al., 2016; Zhu et al., 2016), and that cysteine can coordinate with $Ag^+$ resulting in a reduction in Ag bioavailability and the toxicity of AgNPs and $Ag^+$ (He et al., 2012; Luoma et al., 2016). Thus, the impacts of cysteine on oxidative stress induced by AgNPs and $Ag^+$ were examined in the present work (Fig. 6). In the absence of cysteine, the generation of ROS was significantly stimulated by 1 μM $Ag^+$ and 10 μM AgNPs with respect to the control, but depressed with a further increase in the concentrations of $Ag^+$ and AgNPs to 10 and 100 μM, respectively. It has been documented that the formation of ROS as a natural byproduct occurs during aerobic metabolism in the mitochondria (Chen et al., 2014). The stimulatory induction of ROS in cells at lower doses of $Ag^+$ and AgNPs could be attributed to the fact that the formed ROS were detectable before the toxic effects of AgNPs/$Ag^+$ on mitochondrial functions. On further increasing the AgNP/$Ag^+$ concentrations, however, antioxidant defense systems of *P. chrysosporium* cells would be activated against oxidative damage, leading to ROS scavenging. Similar results were observed under cadmium stress (Chen et al., 2014).

Interestingly, an obvious increasing tendency in ROS generation in a concentration-dependent manner was observed again following the exposure to higher concentrations of $Ag^+$ alone (10–100 μM) relative to the control. Exposure of *P. chrysosporium* cells to single 100 μM $Ag^+$ caused the maximum increase in ROS production, approximately 44-fold higher than that of the control. The results suggested that higher $Ag^+$ concentration exposure evoked overproduction of ROS, eventually resulting in oxidative stress. More surprisingly, cysteine addition elicited a dramatical increase in the ROS level for the samples exposed to 30 μM $Ag^+$ and 100 μM AgNPs. Although the production of ROS was significantly decreased with the addition of 5.0 mM cysteine in the case of cells treated with 100 μM $Ag^+$ as compare to that without cysteine, higher level of ROS production was still obtained. The phenomena reflected that the supplied cysteine led to acceleration or slight mitigation in ROS formation under high AgNP/$Ag^+$ concentrations. It was most likely implicated in the bioavailability of Ag-cysteine complexes, which might be readily taken up into cells, causing irreparable metabolic dysfunction and cell death (Lodeiro et al., 2017). The observations were in line with the cellular viability analysis in the presence of cysteine as shown in Fig. 5b. We have no knowledge of direct evidence for lability and bioavailability of

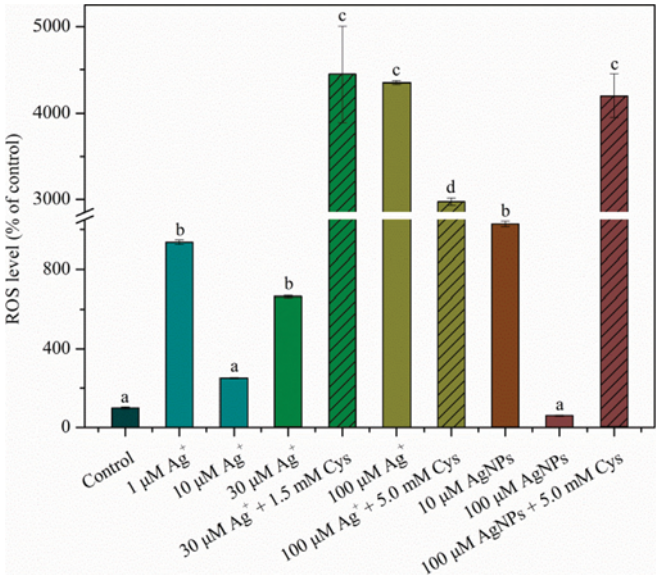


**Fig. 6.** ROS levels of *P. chrysosporium* under AgNP/$Ag^+$ stress in the presence and absence of cysteine.

AgNPs/$Ag^+$-cysteine complexes and further explorations are underway to identify the possible mechanisms involved in bioavailability and contribution of Ag-cysteine complexes to AgNP toxicity towards microbes.

## 4. Conclusion

In addition to enhancement in bioremediation, extracellular protein secretion, and cellular viability, cysteine led to a decrease in total Ag uptake upon exposure to low concentrations of AgNPs and $Ag^+$, especially at a Cys:Ag ratio of 5. More instability in the changing pattern of Ag uptake was observed under stress of AgNPs than $Ag^+$ at this ratio. On the other hand, ROS levels were significantly stimulated by AgNPs and $Ag^+$ in the absence of cysteine, except for the case under high-dose AgNP treatment. After cysteine supplement, prominent stimulatory or marginally alleviatory effects on ROS generation were achieved. Collectively, AgNP/$Ag^+$-induced toxicity to *P. chrysosporium* was enhanced or only marginally mitigated by cysteine, which could be associated with the Cys:Ag ratio and the reactivity of cysteine with AgNPs/$Ag^+$. The insights in this work provide the evidence of no general mechanism for interactions of thiols with AgNPs/$Ag^+$ and have important implications for enhancing understanding of antimicrobial applications and ecotoxicology of AgNPs in natural aquatic systems enriched with organothiols.

## Acknowledgements

This work was financially supported by the National Natural Science Foundation of China (81773333, 51579099, 51521006, and 51508186), the Program for Changjiang Scholars and Innovative Research Team in University (IRT-13R17), and the Hunan Provincial Natural Science Foundation of China (2016JJ3076).

## References

Afshinnia, K., Gibson, I., Merrifeld, R., Baalousha, M., 2016. The concentration-dependent aggregation of AgNPs induced by cystine. Sci. Total Environ. 557–558, 395–403.
Aiken, G.R., Hsu-Kim, H., Ryan, J.N., 2011. Influence of dissolved organic matter on the environmental fate of metals, nanoparticles, and colloids. Environ. Sci. Technol. 45, 3196–3201.
Chen, A., Zeng, G., Chen, G., Liu, L., Shang, C., Hu, X., Lu, L., Chen, M., Zhou, Y., Zhang, Q., 2014. Plasma membrane behavior, oxidative damage, and defense mechanism in *Phanerochaete chrysosporium* under cadmium stress. Process Biochem. 49, 589–598.
Chen, M., Xu, P., Zeng, G., Yang, C., Huang, D., Zhang, J., 2015. Bioremediation of soils contaminated with polycyclic aromatic hydrocarbons, petroleum, pesticides, chlorophenols and heavy metals by composting: applications, microbes and future research needs. Biotechnol. Adv. 33, 745–755.
Cheng, M., Zeng, G., Huang, D., Lai, C., Xu, P., Zhang, C., Liu, Y., 2016. Hydroxyl radicals based advanced oxidation processes (AOPs) for remediation of soils contaminated with organic compounds: a review. Chem. Eng. J. 284, 582–598.
Deng, J.H., Zhang, X.R., Zeng, G.M., Gong, J.L., Niu, Q.Y., Liang, J., 2013. Simultaneous removal of Cd(II) and ionic dyes from aqueous solution using magnetic graphene oxide nanocomposite as an adsorbent. Chem. Eng. J. 226, 189–200.
Dobias, J., Bernier-Latmani, R., 2013. Silver release from silver nanoparticles in natural waters. Environ. Sci. Technol. 47, 4140–4146.
Eckhardt, S., Brunetto, P.S., Gagnon, J., Priebe, M., Giese, B., Fromm, K.M., 2013. Nanobio silver: its interactions with peptides and bacteria, and its uses in medicine. Chem. Rev. 113, 4708–4754.
Ellis, L.J.A., Valsami-Jones, E., Lead, J.R., Baalousha, M., 2016. Impact of surface coating and environmental conditions on the fate and transport of silver nanoparticles in the aquatic environment. Sci. Total Environ. 568, 95–106.
Fabrega, J., Fawcett, S.R., Renshaw, J.C., Lead, J.R., 2009. Silver nanoparticle impact on bacterial growth: effect of pH, concentration, and organic matter. Environ. Sci. Technol. 43, 7285–7290.
Gondikas, A.P., Morris, A., Reinsch, B.C., Marinakos, S.M., Lowry, G.V., Hsu-Kim, H., 2012. Cysteine-induced modifications of zero-valent silver nanomaterials: implications for particle surface chemistry, aggregation, dissolution, and silver speciation. Environ. Sci. Technol. 46, 7037–7045.
Gong, J.L., Wang, B., Zeng, G.M., Yang, C.P., Niu, C.G., Niu, Q.Y., Zhou, W.J., Liang, Y., 2009. Removal of cationic dyes from aqueous solution using magnetic multi-wall carbon nanotube nanocomposite as adsorbent. J. Hazard Mater. 164, 1517–1522.
Guo, Z., Chen, G., Zeng, G., Huang, Z., Chen, A., Hu, L., Wang, J., Jiang, L., 2016a. Cysteine-induced hormesis effect of silver nanoparticles. Toxicol. Res. 5, 1268–1272.
Guo, Z., Chen, G., Zeng, G., Liang, J., Huang, B., Xiao, Z., Yi, F., Huang, Z., He, K., 2016b. Determination of inequable fate and toxicity of Ag nanoparticles in a Phanerochaete chrysosporium biofilm system through different sulfide sources. Environ. Sci. Nano 3, 1027–1035.
He, D., Dorantes-Aranda, J.J., Waite, T.D., 2012. Silver nanoparticle-algae interactions: oxidative dissolution, reactive oxygen species generation and synergistic toxic effects. Environ. Sci. Technol. 46, 8731–8738.
He, K., Chen, G., Zeng, G., Huang, Z., Guo, Z., Huang, T., Peng, M., Shi, J., Hu, L., 2017. Applications of white rot fungi in bioremediation with nanoparticles and biosynthesis of metallic nanoparticles. Appl. Microbiol. Biotechnol. 101, 4853–4862.
Hu, L., Wan, J., Zeng, G., Chen, A., Chen, G., Huang, Z., He, K., Cheng, M., Zhou, C., Xiong, W., Lai, C., Xu, P., 2017. Comprehensive evaluation of the cytotoxicity of CdSe/ZnS quantum dots in *Phanerochaete chrysosporium* by cellular uptake and oxidative stress. Environ. Sci.: Nano 4, 2018–2029.
Hu, L., Zeng, G., Chen, G., Dong, H., Liu, Y., Wan, J., Chen, A., Guo, Z., Yan, M., Wu, H., Yu, Z., 2016. Treatment of landfill leachate using immobilized *Phanerochaete chrysosporium* loaded with nitrogen-doped $TiO_2$ nanoparticles. J. Hazard Mater. 301, 106–118.
Huang, J., Cheng, J., Yi, J., 2016. Impact of silver nanoparticles on marine diatom *Skeletonema costatum*. J. Appl. Toxicol. 36, 1343–1354.
Huang, Z., Chen, G., Zeng, G., Chen, A., Zuo, Y., Guo, Z., Tan, Q., Song, Z., Niu, Q., 2015. Polyvinyl alcohol-immobilized *Phanerochaete chrysosporium* and its application in the bioremediation of composite-polluted wastewater. J. Hazard Mater. 289, 174–183.
Huang, Z., Chen, G., Zeng, G., Guo, Z., He, K., Hu, L., Wu, J., Zhang, L., Zhu, Y., Song, Z., 2017. Toxicity mechanisms and synergies of silver nanoparticles in 2,4-dichlorophenol degradation by *Phanerochaete chrysosporium*. J. Hazard Mater. 321, 37–46.
Huang, Z., Xu, P., Chen, G., Zeng, G., Chen, A., Song, Z., He, K., Yuan, L., Li, H., Hu, L., 2018. Silver ion-enhanced particle-specific cytotoxicity of silver nanoparticles and effect on the production of extracellular secretions of *Phanerochaete chrysosporium*. Chemosphere 196, 575–584.
Kanel, S.R., Flory, J., Meyerhoefer, A., Fraley, J.L., Sizemore, I.E., Goltz, M.N., 2015. Influence of natural organic matter on fate and transport of silver nanoparticles in saturated porous media: laboratory experiments and modeling. J. Nanopart. Res. 17, 154.
Khan, S.S., Srivatsan, P., Vaishnavi, N., Mukherjee, A., Chandrasekaran, N., 2011. Interaction of silver nanoparticles (SNPs) with bacterial extracellular proteins (ECPs) and its adsorption isotherms and kinetics. J. Hazard Mater. 192, 299–306.
Khojasteh, V.J., Alfakhri, S., Foster, H.A., 2016. Effects of silver sulphadiazine on production of extracellular proteins by strains of *Staphylococcus aureus* isolated from burns wound. Iran. J. Pharm. Res. 15, 653–660.
Li, C.C., Wang, Y.J., Dang, F., Zhou, D.M., 2016. Mechanistic understanding of reduced AgNP phytotoxicity induced by extracellular polymeric substances. J. Hazard Mater. 308, 21–28.
Liang, J., Yang, Z., Tang, L., Zeng, G., Yu, M., Li, X., Wu, H., Qian, Y., Li, X., Luo, Y., 2017. Changes in heavy metal mobility and availability from contaminated wetland soil remediated with combined biochar-compost. Chemosphere 181, 281–288.
Liu, J., Sonshine, D.A., Shervani, S., Hurt, R.H., 2010. Controlled release of biologically active silver from nanosilver surfaces. ACS Nano 4, 6903–6913.
Lodeiro, P., Browning, T.J., Achterberg, E.P., Guillou, A., El-Shahawi, M.S., 2017. Mechanisms of silver nanoparticle toxicity to the coastal marine diatom *Chaetoceros curvisetus*. Sci. Rep. 7, 10777.
Long, F., Gong, J.L., Zeng, G.M., Chen, L., Wang, X.Y., Deng, J.H., Niu, Q.Y., Zhang, H.Y., Zhang, X.R., 2011. Removal of phosphate from aqueous solution by magnetic Fe-Zr binary oxide. Chem. Eng. J. 171, 448–455.
Luoma, S.N., Stoiber, T., Croteau, M.N., Römer, I., Merrifeld, R., Lead, J., 2016. Effect of cysteine and humic acids on bioavailability of Ag from Ag nanoparticles to a freshwater snail. NanoImpact 2, 61–69.
Massarsky, A., Trudeau, V.L., Moon, T.W., 2014. Predicting the environmental impact of nanosilver. Environ. Toxicol. Pharmacol. 38, 861–873.
Navarro, E., Piccapietra, F., Wagner, B., Marconi, F., Kaegi, R., Odzak, N., Sigg, L., Behra, R., 2008. Toxicity of silver nanoparticles to *Chlamydomonas reinhardtii*. Environ. Sci. Technol. 42, 8959–8964.
Navarro, E., Wagner, B., Odzak, N., Sigg, L., Behra, R., 2015. Effects of differently coated silver nanoparticles on the photosynthesis of *Chlamydomonas reinhardtii*. Environ. Sci. Technol. 49, 8041–8047.
Priester, J.H., Singhal, A., Wu, B., Stucky, G.D., Holden, P.A., 2014. Integrated approach to evaluating the toxicity of novel cysteine-capped silver nanoparticles to *Escherichia coli* and *Pseudomonas aeruginosa*. Analyst 139, 954–963.
Ren, X., Zeng, G., Tang, L., Wang, J., Wan, J., Liu, Y., Yu, J., Yi, H., Ye, S., Deng, R., 2017. Sorption, transport and biodegradation - an insight into bioavailability of persistent organic pollutants in soil. Sci. Total Environ. 610–611, 1154–1163.
Siriwardana, K., Suwandaratne, N., Perera, G.S., Collier, W.E., Perez, F., Zhang, D.M., 2015a. Contradictory dual effects: organothiols can induce both silver nanoparticle disintegration and formation under ambient conditions. J. Phys. Chem. C 119, 20975–20984.
Siriwardana, K., Wang, A., Gadogbe, M., Collier, W.E., Fitzkee, N.C., Zhang, D., 2015b. Studying the effects of cysteine residues on protein interactions with silver nanoparticles. J. Phys. Chem. C 119, 2910–2916.

Stoiber, T., Croteau, M.N., Römer, I., Tejamaya, M., Lead, J.R., Luoma, S.N., 2015. Influence of hardness on the bioavailability of silver to a freshwater snail after waterborne exposure to silver nitrate and silver nanoparticles. Nanotoxicology 9, 918–927.

Tan, X., Liu, Y., Zeng, G., Wang, X., Hu, X., Gu, Y., Yang, Z., 2015. Application of biochar for the removal of pollutants from aqueous solutions. Chemosphere 125, 70–85.

Tang, W.W., Zeng, G.M., Gong, J.L., Liang, J., Xu, P., Zhang, C., Huang, B.B., 2014. Impact of humic/fulvic acid on the removal of heavy metals from aqueous solutions using nanomaterials: a review. Sci. Total Environ. 468–469, 1014–1027.

Wan, J., Zeng, G., Huang, D., Hu, L., Xu, P., Huang, C., Deng, R., Xue, W., Lai, C., Zhou, C., Zheng, K., Ren, X., Gong, X., 2017. Rhamnolipid stabilized nanochlorapatite: synthesis and enhancement effect on Pb-and Cd-immobilization in polluted sediment. J. Hazard Mater. 343, 332–339.

Wang, Y.W., Tang, H., Wu, D., Liu, D., Liu, Y.F., Cao, A.N., Wang, H.F., 2016. Enhanced bactericidal toxicity of silver nanoparticles by the antibiotic gentamicin. Environ. Sci. Nano 3, 788–798.

Wirth, S.M., Lowry, G.V., Tilton, R.D., 2012. Natural organic matter alters biofilm tolerance to silver nanoparticles and dissolved silver. Environ. Sci. Technol. 46, 12687–12696.

Wu, H., Lai, C., Zeng, G., Liang, J., Chen, J., Xu, J., Dai, J., Li, X., Liu, J., Chen, M., Lu, L., Hu, L., Wan, J., 2017. The interactions of composting and biochar and their implications for soil amendment and pollution remediation: a review. Crit. Rev. Biotechnol. 37, 754–764.

Xiu, Z.M., Ma, J., Alvarez, P.J.J., 2011. Differential effect of common ligands and molecular oxygen on antimicrobial activity of silver nanoparticles versus silver ions. Environ. Sci. Technol. 45, 9003–9008.

Xiu, Z.M., Zhang, Q.B., Puppala, H.L., Colvin, V.L., Alvarez, P.J.J., 2012. Negligible particle-specific antibacterial activity of silver nanoparticles. Nano Lett. 12, 4271–4275.

Xu, P., Zeng, G.M., Huang, D.L., Feng, C.L., Hu, S., Zhao, M.H., Lai, C., Wei, Z., Huang, C., Xie, G.X., Liu, Z.F., 2012a. Use of iron oxide nanomaterials in wastewater treatment: a review. Sci. Total Environ. 424, 1–10.

Xu, P., Zeng, G.M., Huang, D.L., Lai, C., Zhao, M.H., Wei, Z., Li, N.J., Huang, C., Xie, G.X., 2012b. Adsorption of Pb(II) by iron oxide nanoparticles immobilized *Phanerochaete chrysosporium*: equilibrium, kinetic, thermodynamic and mechanisms analysis. Chem. Eng. J. 203, 423–431.

Yang, X., Jiang, C., Hsu-Kim, H., Badireddy, A.R., Dykstra, M., Wiesner, M., 2014. Silver nanoparticle behavior, uptake, and toxicity in *Caenorhabditis elegans*: effects of natural organic matter. Environ. Sci. Technol. 48, 3486–3495.

Yuan, X., Wang, H., Wu, Y., Zeng, G., Chen, X., Leng, L., Wu, Z., Li, H., 2016. One-pot self-assembly and photoreduction synthesis of silver nanoparticle-decorated reduced graphene oxide/MIL-125(Ti) photocatalyst with improved visible light photocatalytic activity. Appl. Organometal. Chem. 30, 289–296.

Yi, F., Chen, G., Zeng, G., Guo, Z., Liu, W., Huang, Z., He, K., Hu, L., 2016. Influence of cysteine and bovine serum albumin on silver nanoparticle stability, dissolution, and toxicity to *Phanerochaete chrysosporium*. RSC Adv. 6, 106177–106185.

Zhang, C., Lai, C., Zeng, G., Huang, D., Yang, C., Wang, Y., Zhou, Y., Cheng, M., 2016. Efficacy of carbonaceous nanocomposites for sorbing ionizable antibiotic sulfamethazine from aqueous solution. Water Res. 95, 103–112.

Zhang, J., Wang, F., House, J.D., Page, B., 2004. Thiols in wetland interstitial waters and their role in mercury and methylmercury speciation. Limnol. Oceanogr. 49, 2276–2286.

Zhang, L., Yuan, X., Wang, H., Chen, X., Wu, Z., Liu, Y., Gu, S., Jiang, Q., Zeng, G., 2015a. Facile preparation of Ag/$AgVO_3$/BiOCl composite and its enhanced photocatalytic behavior for methylene blue degradation. RSC Adv. 5, 98184–98193.

Zhang, Y., Zeng, G.M., Tang, L., Chen, J., Zhu, Y., He, X.X., He, Y., 2015b. Electrochemical sensor based on electrodeposited graphene-au modified electrode and nanoau Carrier amplified signal strategy for attomolar mercury detection. Anal. Chem. 87, 989–996.

Zhou, C., Lai, C., Huang, D., Zeng, G., Zhang, C., Cheng, M., Hu, L., Wan, J., Xiong, W., Wen, M., Wen, X., Qin, L., 2018. Highly porous carbon nitride by supramolecular preassembly of monomers for photocatalytic removal of sulfamethazine under visible light driven. Appl. Catal. B 220, 202–210.

Zhu, B., Li, Y., Lin, Z., Zhao, M., Xu, T., Wang, C., Deng, N., 2016. Silver nanoparticles induce HePG-2 cells apoptosis through ROS-mediated signaling pathways. Nanoscale Res. Lett. 11, 198.

Zuo, Y., Chen, G., Zeng, G., Li, Z., Yan, M., Chen, A., Guo, Z., Huang, Z., Tan, Q., 2015. Transport fate, and stimulating impact of silver nanoparticles on the removal of Cd(II) by *Phanerochaete chrysosporium* in aqueous solutions. J. Hazard Mater. 285, 236–244.